ISSN 1392 - 1207. MECHANIKA. 2013 Volume 19(4): 380-389

Navier-type bending analysis of general composite laminates under different types of thermomechanical loading

M.A. Torabizadeh*, A. Fereidoon**
**University of Applied Science and Technology, Tehran, Iran. E-mail: torabizadeh@uast.ac.ir*
***Mechanical Engineering Department, University of Semnan, Semnan, Iran. E-mail: afereidoon@semnan.ac.ir*
crossref http://dx.doi.org/10.5755/j01.mech.19.4.5052

1. Introduction

Due to the wide spread applications in engineering structures, composite members are receiving more attentions from the research communities, since they are stronger, stiffer, and more ductile than the sum of the individual elements. Analysis of deformation and stress fields in composite laminates is of fundamental importance in experimental determination of the lamina properties and exact solutions are useful in developing a numerical model. Zhang et al. [1] illustrated a new procedure for obtaining the static exact solution of composite laminates with piezo-thermo-elastic layers under cylindrical bending. Duc and Minh [3] presented a method to determine bending deflection of three-phase polymer composite plates consisting of reinforced glass fibers and titanium oxide particles. An investigation of the stochastic nonlinear bending response of a laminated composite plate resting on a two parameter Pastemak elastic foundation with Winkler cubic nonlinearity subjected to transverse distributed static load was given by Singh et al. [4]. Sturzenbecher and Hofstetter [5] analyzed bending response of cross-ply laminated composites based on models of Lekhnitskii and Ren. Cetkovic and Vuksanovic [6] used an original MATLAB computer code to perform finite element solution for bending, free vibrations and buckling of laminated composite and sandwich plates using a layerwise displacement model. Dash and Singh [7] used a higher order shear deformation theory to investigate a transverse bending of laminated composite plates in Green-Lagrange sense accounting for the transverse shear and large rotations. Shiyekar and Kant [9] applied higher order shear deformation theory to analyze piezoelectric fiber reinforced composites under bi-directional bending. Higher order shear and normal deformable plate theory and a meshless method was used by Xiao et al. [10] to analyze static infinitesimal deformations of thick laminated composite elastic plates under different boundary conditions. Kant and Swaminathan [13] also used higher order refined theory to present an analytical solution to static loading of simply supported composite and sandwich plates. Andrade et al. [8] presented geometrically nonlinear static and dynamic analysis of laminated composite plates and shells using the eight-node hexahedral element with one-point integration and compared outputs with results obtained by other authors using different element types. Xu and Wu [11] illustrated a two-dimensional analytical solution for simply supported composite beams with interlayer slips by consideration of shear deformation effects. Kant et al. [12] presented a novel semi-analytical model for accurate estimation of stresses and displacements in composite and sandwich laminates. Their results were seen to compare well with the available three dimensional elasticity and analytical solutions. Shen [2] give the nonlinear analysis for bending of simply supported functionally graded nanocomposite plates subjected to a transverse uniform or sinusoidal loads in thermal environments. For this purpose, he used a higher order theory to derive governing equations. Also Mousavi and Tahani [14] presented an analytical solution for bending of moderately thick radially functionally graded sector plates with general boundary conditions using Kantorovich method.

In spite of the abundant literature on the subject, the choice of mechanical response of composite plates under different types of loading in thermal environments with general configuration and boundary condition is critical issues. Classical lamination theory is used to derive governing equations and the Navier-type solution is applied to solve them for simply supported boundary conditions. Three types of mechanical loadings and two types of thermal distribution are considered to investigate the effect of loading, temperature service, geometry ratio and mechanical properties on static bending of laminated composites. A finite element code using ANSYS is also developed to evaluate accuracy of the presented solution.

2. Theoretical formulation

2.1. Displacement and strains

A rectangular plate of sides *a* and *b* with thickness *h*, shown in Fig. 1.

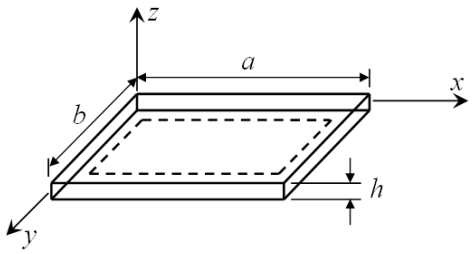

Fig. 1 Geometry of simply supported rectangular laminated plates used in the analytical solutions

Based on classical lamination plate theory, the following displacement field can be assumed:

$$u(x,y,z)=u_0(x,y)-z\frac{\partial\omega_0}{\partial x}; \tag{1}$$

$$v(x,y,z)=v_0(x,y)-z\frac{\partial\omega_0}{\partial y}; \tag{2}$$

$$\omega(x,y,z)=\omega_0(x,y), \tag{3}$$

where u_0, v_0, w_0 are the displacements along the coordinate lines of a material point on xy-plane.

The von Karman strains associated with the displacement field in static loading can be computed using the strain-displacement relations for small strains:

$$\left.\begin{aligned}
&\varepsilon_{xx}=\frac{\partial u_0}{\partial x}-z\frac{\partial^2\omega_0}{\partial x^2};\ \ \varepsilon_{yy}=\frac{\partial v_0}{\partial y}-z\frac{\partial^2\omega_0}{\partial y^2};\\
&\varepsilon_{xy}=\frac{1}{2}\left(\frac{\partial u_0}{\partial y}+\frac{\partial v_0}{\partial x}\right)-z\frac{\partial^2\omega_0}{\partial x\partial y};\\
&\varepsilon_{xz}=\varepsilon_{yz}=\varepsilon_{zz}=0.
\end{aligned}\right\} \tag{4}$$

Note that the transverse strains are identically zero in classical plate theory. The first three strains have the form:

$$\begin{Bmatrix}\varepsilon_{xx}\\ \varepsilon_{yy}\\ \varepsilon_{xy}\end{Bmatrix}=\begin{Bmatrix}\varepsilon^0_{xx}\\ \varepsilon^0_{yy}\\ \varepsilon^0_{xy}\end{Bmatrix}+z\begin{Bmatrix}\varepsilon^1_{xx}\\ \varepsilon^1_{yy}\\ \varepsilon^1_{xy}\end{Bmatrix}. \tag{5}$$

If the temperature increment varies linearly, consistent with the mechanical strains, we can write:

$$\Delta T(x,y,z)=T_0(x,y)+zT_1(x,y). \tag{6}$$

And the total strains are of the form:

$$\begin{Bmatrix}\varepsilon_{xx}\\ \varepsilon_{yy}\\ \varepsilon_{xy}\end{Bmatrix}=\begin{Bmatrix}\varepsilon^0_{xx}\\ \varepsilon^0_{yy}\\ \varepsilon^0_{xy}\end{Bmatrix}+z\begin{Bmatrix}\varepsilon^1_{xx}\\ \varepsilon^1_{yy}\\ \varepsilon^1_{xy}\end{Bmatrix}=$$
$$=\begin{Bmatrix}\varepsilon^0_{xx}-\alpha_{xx}T_0\\ \varepsilon^0_{yy}-\alpha_{yy}T_0\\ \varepsilon^0_{xy}-2\alpha_{xy}T_0\end{Bmatrix}+z\begin{Bmatrix}\varepsilon^1_{xx}-\alpha_{xx}T_1\\ \varepsilon^1_{yy}-\alpha_{yy}T_1\\ \varepsilon^1_{xy}-2\alpha_{xy}T_1\end{Bmatrix}. \tag{7}$$

2.2. Equilibrium equations

By using Eqs. (7) and (4) the constitutive equations are obtained as follows:

$$\begin{Bmatrix}N_{xx}\\ N_{yy}\\ N_{xy}\end{Bmatrix}=\begin{bmatrix}A_{11}&A_{12}&A_{16}\\ A_{21}&A_{22}&A_{26}\\ A_{61}&A_{62}&A_{66}\end{bmatrix}\begin{Bmatrix}\varepsilon^0_{xx}\\ \varepsilon^0_{yy}\\ \varepsilon^0_{xy}\end{Bmatrix}+\begin{bmatrix}B_{11}&B_{12}&B_{16}\\ B_{21}&B_{22}&B_{26}\\ B_{61}&B_{62}&B_{66}\end{bmatrix}\begin{Bmatrix}\varepsilon^1_{xx}\\ \varepsilon^1_{yy}\\ \varepsilon^1_{xy}\end{Bmatrix}-\begin{Bmatrix}N^T_{xx}\\ N^T_{yy}\\ N^T_{xy}\end{Bmatrix}; \tag{8}$$

$$\begin{Bmatrix}M_{xx}\\ M_{yy}\\ M_{xy}\end{Bmatrix}=\begin{bmatrix}B_{11}&B_{12}&B_{16}\\ B_{21}&B_{22}&B_{26}\\ B_{61}&B_{62}&B_{66}\end{bmatrix}\begin{Bmatrix}\varepsilon^0_{xx}\\ \varepsilon^0_{yy}\\ \varepsilon^0_{xy}\end{Bmatrix}+\begin{bmatrix}D_{11}&D_{12}&D_{16}\\ D_{21}&D_{22}&D_{26}\\ D_{61}&D_{62}&D_{66}\end{bmatrix}\begin{Bmatrix}\varepsilon^1_{xx}\\ \varepsilon^1_{yy}\\ \varepsilon^1_{xy}\end{Bmatrix}-\begin{Bmatrix}M^T_{xx}\\ M^T_{yy}\\ M^T_{xy}\end{Bmatrix}, \tag{9}$$

where A_{ij} are extensional stiffnesses, D_{ij} the bending stiffnesses and B_{ij} the bending-extensional coupling stiffnesses, which are defined in terms of the transformed laminate stiffnesses $\bar{Q}_{ij}$ as:

$$\left(A_{ij},B_{ij},D_{ij}\right)=\int_{-\frac{h}{2}}^{\frac{h}{2}}\bar{Q}_{ij}\left(1,z,z^2\right)dz. \tag{10}$$

Also $\{N^T\}$ and $\{M^T\}$ are thermal force resultants:

$$\{N^T\}=\sum_{k=1}^{N}\int_{z_k}^{z_{k+1}}\left[\bar{Q}\right]^k\{\bar{\alpha}\}^k\,\Delta T\ \ dz; \tag{11}$$

$$\{M^T\}=\sum_{k=1}^{N}\int_{z_k}^{z_{k+1}}\left[\bar{Q}\right]^k\{\bar{\alpha}\}^k\,\Delta T\ z\,dz. \tag{12}$$

Equations of equilibrium can be derived using variational principle which is not explained in details here (see [15]). Three equilibrium equations are as follows:

$$\delta u_0:\ \frac{\partial N_{xx}}{\partial x}+\frac{\partial N_{xy}}{\partial y}=0; \tag{13}$$

$$\delta v_0:\ \frac{\partial N_{xy}}{\partial x}+\frac{\partial N_{yy}}{\partial y}=0; \tag{14}$$

$$\delta\omega_0:\ \frac{\partial^2 M_{xx}}{\partial x^2}+2\frac{\partial^2 M_{xy}}{\partial x\partial y}+\frac{\partial^2 M_{yy}}{\partial y^2}+N(\omega_0)+q=0, \tag{15}$$

where

$$N(\omega_0)=\frac{\partial}{\partial x}\left(N_{xx}\frac{\partial\omega_0}{\partial x}+N_{xy}\frac{\partial\omega_0}{\partial y}\right)+$$
$$+\frac{\partial}{\partial y}\left(N_{xy}\frac{\partial\omega_0}{\partial x}+N_{yy}\frac{\partial\omega_0}{\partial y}\right). \tag{16}$$

2.3. Boundary conditions

The Navier solutions can be developed for rectangular laminates with two sets of simply supported boundary conditions. Even for these boundary conditions, not all laminates permit the Navier solution. The two types of simply supported boundary conditions on the displacements and stress resultants used in classical lamination plate theory (CLPT) are given below [15].

Simply supported (SS-1):

$$\left.\begin{array}{l} u_0(x,0)=0;\ u_0(x,b)=0;\ v_0(0,y)=0;\ v_0(a,y)=0;\quad \omega_0(a,y)=0;\ \omega_0(0,y)=0;\quad \omega_0(x,0)=0;\quad \omega_0(x,b)=0; \\ \left.\frac{\partial\omega_0}{\partial x}\right|_{(x,0)}=0;\ \left.\frac{\partial\omega_0}{\partial x}\right|_{(x,b)}=0;\ \left.\frac{\partial\omega_0}{\partial y}\right|_{(0,y)}=0;\quad \left.\frac{\partial\omega_0}{\partial y}\right|_{(a,y)}=0; N_{xx}(0,y)=0; N_{xx}(a,y)=0; N_{yy}(x,0)=0; \\ N_{yy}(x,b)=0; M_{yy}(x,b)=0; M_{yy}(x,0)=0; M_{xx}(0,y)=0; M_{xx}(a,y)=0. \end{array}\right\} \quad (17)$$

Simply supported (SS-2):

$$\left.\begin{array}{l} u_0(0,y)=0;\ u_0(a,y)=0;\ v_0(x,0)=0;\ v_0(x,b)=0;\ \omega_0(a,y)=0;\ \omega_0(0,y)=0;\ \omega_0(x,0)=0;\ \omega_0(x,b)=0; \\ \left.\frac{\partial\omega_0}{\partial x}\right|_{(x,0)}=0;\ \left.\frac{\partial\omega_0}{\partial x}\right|_{(x,b)}=0;\ \left.\frac{\partial\omega_0}{\partial y}\right|_{(0,y)}=0;\ \left.\frac{\partial\omega_0}{\partial y}\right|_{(a,y)}=0; N_{xy}(0,y)=0;\ N_{xy}(a,y)=0;\ N_{xy}(x,0)=0; \\ N_{xy}(x,b)=0;\ M_{yy}(x,b)=0; M_{yy}(x,0)=0; M_{xx}(0,y)=0;\ M_{xx}(a,y)=0. \end{array}\right\} \quad (18)$$

The Navier solutions using SS-1 boundary conditions can be obtained only for laminates whose stiffnesses A_{16}, A_{26}, B_{16}, B_{26}, D_{l6}, D_{26}, and A_{45} are zero. Thus, the Navier solutions for the SS-1 boundary conditions can be developed for laminates with a single generally orthotropic layer, symmetrically laminated plates with multiple specially orthotropic layers, and antisymmetric cross-ply laminated plates. Similarly, the Navier solutions using SS-2 boundary conditions can be obtained only for laminates whose stiffnesses A_{16}, A_{26}, B_{11}, B_{12}, B_{22}, B_{66}, D_{16}, D_{26}, and A_{45} are zero, i.e., for laminates with a single generally orthotropic layer, symmetrically laminated plates with multiple specially orthotropic layers, and antisymmetric angle-ply laminated plates. [15]. In all cases of this study, nonlinear terms are omitted.

2.4. Navier solution methodology

The displacement boundary conditions of simply supported in (17-18) are satisfied by assuming the following form of the displacements:

$$u_0(x,y)=\sum_{n=1}^{\infty}\sum_{m=1}^{\infty}U_{mn}\cos\alpha x\ \sin\beta y; \quad (19)$$

$$v_0(x,y)=\sum_{n=1}^{\infty}\sum_{m=1}^{\infty}V_{mn}\sin\alpha x\ \cos\beta y; \quad (20)$$

$$\omega_0(x,y)=\sum_{n=1}^{\infty}\sum_{m=1}^{\infty}W_{mn}\sin\alpha x\sin\beta y, \quad (21)$$

where $\alpha=m\pi/a$ and $\beta=n\pi/b$ and U_{mn},V_{mn},W_{mn} are coefficients to be determined.

Considerations of Eqs. (19)-(21), shows that the mechanical transverse load q and thermal forces should also be expanded in double sine series. Thus:

$$q(x,y)=\sum_{n=1}^{\infty}\sum_{m=1}^{\infty}Q_{mn}\ \sin\alpha x\ \sin\beta y; \quad (22)$$

$$Q_{mn}=\frac{4}{ab}\int_0^a\int_0^b q(x,y)\sin\alpha x\ \sin\beta y\ dxdy. \quad (23)$$

And the temperature increment is expanded as:

$$\Delta T(x,y,z)=\sum_{n=1}^{\infty}\sum_{m=1}^{\infty}T_{mn}(\mathrm{z})\ \sin\alpha x\ \sin\beta y; \quad (24)$$

$$T_{mn}(z)=\frac{4}{ab}\int_0^a\int_0^b\Delta T(x,y,z)\ \sin\alpha x\ \sin\beta y\ dxdy. \quad (25)$$

Then thermal force and moment resultants can be assumed as:

$$\begin{Bmatrix}N_{xx}^T\\N_{yy}^T\\N_{xy}^T\end{Bmatrix}=\sum_{n=1}^{\infty}\sum_{m=1}^{\infty}\begin{Bmatrix}N_{mn}^1\\N_{mn}^2\\N_{mn}^6\end{Bmatrix}\sin\alpha x\ \sin\beta y; \quad (26)$$

$$\begin{Bmatrix}M_{xx}^T\\M_{yy}^T\\M_{xy}^T\end{Bmatrix}=\sum_{n=1}^{\infty}\sum_{m=1}^{\infty}\begin{Bmatrix}M_{mn}^1\\M_{mn}^2\\M_{mn}^6\end{Bmatrix}\sin\alpha x\ \sin\beta y, \quad (27)$$

where

$$\{N_{mn}\}=\sum_{k=1}^{N}\int_{z_k}^{z_{k+1}}\left[\bar{Q}\right]^k\{\bar{\alpha}\}^k T_{mn}(z)\ dz; \quad (28)$$

$$\{M_{mn}\}=\sum_{k=1}^{N}\int_{z_k}^{z_{k+1}}\left[\bar{Q}\right]^k\{\bar{\alpha}\}^k T_{mn}(z)\ \mathrm{z}\ dz. \quad (29)$$

By expansion of generalized displacements and loads in a double trigonometric series in terms of unknown parameters, Eqs. (13)-(15) can be cast in differential operator form:

$$\begin{bmatrix}c_{11}&c_{12}&c_{13}\\c_{12}&c_{22}&c_{23}\\c_{13}&c_{23}&c_{33}\end{bmatrix}\begin{Bmatrix}u_0\\v_0\\\omega_0\end{Bmatrix}=\begin{Bmatrix}0\\0\\q\end{Bmatrix}+\begin{Bmatrix}f_1^T\\f_2^T\\f_3^T\end{Bmatrix}, \quad (30)$$

where coefficients c_{ij} are defined by:

$$\left.\begin{aligned}
&c_{11}=A_{11}\frac{\partial^2}{\partial x^2}+2A_{16}\frac{\partial}{\partial x}\frac{\partial}{\partial y}+A_{66}\frac{\partial^2}{\partial y^2};\ c_{12}=A_{16}\frac{\partial^2}{\partial x^2}+\left(A_{12}+A_{66}\right)\frac{\partial}{\partial x}\frac{\partial}{\partial y}+A_{26}\frac{\partial^2}{\partial y^2};\\
&c_{13}=-\left[B_{11}\frac{\partial^3}{\partial x^3}+3B_{16}\frac{\partial^2}{\partial x^2}\frac{\partial}{\partial y}+\left(B_{12}+2B_{66}\right)\frac{\partial}{\partial x}\frac{\partial^2}{\partial y^2}+B_{26}\frac{\partial^3}{\partial y^3}\right];\\
&c_{22}=A_{66}\frac{\partial^2}{\partial x^2}+2A_{26}\frac{\partial}{\partial x}\frac{\partial}{\partial y}+A_{22}\frac{\partial^2}{\partial y^2};\ c_{23}=-\left[B_{16}\frac{\partial^3}{\partial x^3}+3B_{26}\frac{\partial}{\partial x}\frac{\partial^2}{\partial y^2}+\left(B_{12}+2B_{66}\right)\frac{\partial^2}{\partial x^2}\frac{\partial}{\partial y}-B_{22}\frac{\partial^3}{\partial y^3}\right];\\
&c_{33}=D_{11}\frac{\partial^4}{\partial x^4}+4D_{16}\frac{\partial^3}{\partial x^3}\frac{\partial}{\partial y}+2\left(D_{12}+2D_{66}\right)\frac{\partial^2}{\partial x^2}\frac{\partial^2}{\partial y^2}+4D_{26}\frac{\partial}{\partial x}\frac{\partial^3}{\partial y^3}+D_{22}\frac{\partial^4}{\partial y^4}.
\end{aligned}\right\}\quad(31)$$

Coefficients f_i^T are defined by:

$$\left.\begin{aligned}
&f_1^T=\frac{\partial N_{xx}^T}{\partial x}+\frac{\partial N_{xy}^T}{\partial y};\ f_2^T=\frac{\partial N_{xy}^T}{\partial x}+\frac{\partial N_{yy}^T}{\partial y};\\
&f_3^T=-\left(\frac{\partial^2 M_{xx}^T}{\partial x^2}+2\frac{\partial^2 M_{xy}^T}{\partial y\partial x}+\frac{\partial^2 M_{yy}^T}{\partial y^2}\right).
\end{aligned}\right\}\quad(32)$$

Eq. (30) are solved using the method of static condensation. This method allows the elimination of a selected set of variables and retains a desired set of variables. In order to this, the coefficients associated with the in-plane displacements are eliminated and those related with the transverse deflection are retained. Finally coefficients of unknown U_{mn}, V_{mn}, W_{mn} are determined. (for more details about this method, see Ref. [15]) Solution of Eq. (30) for each *m*, *n* = 1, 2,… gives U_{mn}, V_{mn}, W_{mn}, which can be used to compute the final solution.

2.5. Determination of stresses

The in-plane stresses in each layer of a laminate are calculated from constitutive relations. Accounting for mechanical and thermal effects:

$$\begin{Bmatrix}\sigma_{xx}\\ \sigma_{yy}\\ \sigma_{xy}\end{Bmatrix}^k=\begin{bmatrix}\bar{Q}_{11} & \bar{Q}_{12} & \bar{Q}_{16}\\ \bar{Q}_{12} & \bar{Q}_{22} & \bar{Q}_{26}\\ \bar{Q}_{16} & \bar{Q}_{26} & \bar{Q}_{66}\end{bmatrix}^k\left(\begin{Bmatrix}\varepsilon_{xx}\\ \varepsilon_{yy}\\ 2\varepsilon_{xy}\end{Bmatrix}-\begin{Bmatrix}\alpha_{xx}\\ \alpha_{yy}\\ 2\alpha_{xy}\end{Bmatrix}\Delta T\right).\quad(33)$$

The transverse stresses in a laminate can be determined using the 3-D equilibrium equations for any $z_k \le z \le z_{k+1}$:

$$\sigma_{xz}^k=-\int_{z_k}^{z}\left(\frac{\partial\sigma_{xx}^k}{\partial x}+\frac{\partial\sigma_{xy}^k}{\partial y}\right)dz+C_1^k(x,y);\quad(34)$$

$$\sigma_{yz}^k=-\int_{z_k}^{z}\left(\frac{\partial\sigma_{xy}^k}{\partial x}+\frac{\partial\sigma_{yy}^k}{\partial y}\right)dz+C_2^k(x,y);\quad(35)$$

$$\sigma_{xz}^k=-\int_{z_k}^{z}\left(\frac{\partial\sigma_{xz}^k}{\partial x}+\frac{\partial\sigma_{yz}^k}{\partial y}\right)dz+C_3^k(x,y),\quad(36)$$

where $\sigma_{xx}^k, \sigma_{yy}^k$ and σ_{xy}^k are known from Eq. (33) and C_i^k are functions to be determined using the boundary conditions and continuity of stresses at layer interfaces.

3. Results and discussion

3.1. Mechanical loading

In all examples, material properties of the plate are assumed as:

$$\frac{E_{11}}{E_{22}}=25,\ \frac{G_{12}}{E_{22}}=\frac{G_{13}}{E_{22}}=0.5,\ \frac{G_{23}}{E_{22}}=0.2,\ \upsilon_{12}=0.3.\quad(37)$$

In this study, three types of loads including uniform, center point and sinusoidal distributed loads in mechanical loading are considered.

Uniform distributed load (UDL): $q(x,y)=Q_0$.

Center point load (CPL):

$$q(x,y)=Q_0\ \text{ at }\ x=a/2,\ y=b/2.\quad(38)$$

Sinusoidal distributed load (SSL):

$$q(x,y)=Q_0\sin(\pi x/a)\cos(\pi y/b).$$

The length-to-thickness ratio (i.e., *a*/*h*) is assumed to be 10 in all numerical examples. Furthermore, in the mechanical loading results the various non-dimensionalized parameters used are:

$$\left.\begin{aligned}
&\text{deflection: } \bar{\omega}=\left(\omega\, E_2\, h^3/Q_0\, a^4\right);\\
&\text{shear stress: } \bar{\sigma}_{xz}=\left(\sigma_{xy}\, h/Q_0\, b\right);\\
&\text{transverse stress: } \bar{\sigma}_{yy}=\left(\sigma_{yy}\, h^2/Q_0\, a^2\right);\\
&\text{longitudinal stress: } \bar{\sigma}_{xx}=\left(\sigma_{xx}\, h^2/Q_0\, b^2\right).
\end{aligned}\right\}\quad(39)$$

All results presented in this section are compared with results of other numerical and analytical studies available in the literature as well as those obtained from the commercial finite element code ANSYS. Composite plates have been modeled in ANSYS by using three-dimensional 8-node layered elements which allows up to 250 different material layers in the thickness direction in each element without much increase of counting time. Mechanical properties of a unidirectional laminate at room temperature are used as initial values in finite element method. In this model, manual mesh is used and also the mesh is refined till no significant change in displacements and stresses are obtained. As mentioned before, the simply supported boundary conditions (SS-1) place a restriction on the laminate scheme of composite plates. First cross-ply lamination is selected for both mechanical and thermal loading.

Table 1

Transverse deflections and stresses in square laminates subjected to uniformly distributed transverse load (UDL), sinusoidal load (SSL) or central point load (CPL)*

$(0/90)_k$		UDL				SSL				CPL			
		$\bar{\omega}\times10^2$	$\bar{\sigma}_{xx}$	$\bar{\sigma}_{yy}$	$\bar{\sigma}_{xy}$	$\bar{\omega}\times10^2$	$\bar{\sigma}_{xx}$	$\bar{\sigma}_{yy}$	$\bar{\sigma}_{xy}$	$\bar{\omega}\times10^2$	$\bar{\sigma}_{xx}$	$\bar{\sigma}_{yy}$	$\bar{\sigma}_{xy}$
k = 1	Analytical	1.614	0.148	1.174	0.079	0.995	0.086	0.724	0.049	3.989	0.759	6.087	0.196
	FEM	1.734	0.156	1.186	0.083	1.062	0.092	0.733	0.051	4.087	0.798	6.819	0.199
	Reddy [15]	1.695	0.126	1.076	0.093	1.063	0.084	0.715	0.052	4.666	0.801	6.821	0.193
	Diff, %	6.92	5.40	1.02	5.06	6.73	6.97	1.24	4.08	2.45	5.13	12.02	1.53
k = 2	Analytical	0.763	0.059	0.792	0.037	0.470	0.036	0.489	0.023	1.910	0.291	4.265	0.091
	FEM	0.801	0.061	0.826	0.039	0.510	0.038	0.490	0.025	2.029	0.302	4.386	0.096
	Reddy [15]	0.808	0.054	0.736	0.044	0.506	0.035	0.486	0.025	2.210	0.329	4.495	0.093
	Diff, %	4.98	3.38	4.29	5.40	8.51	5.55	0.20	8.69	6.23	3.78	2.83	5.49
k = 4	Analytical	0.674	0.049	0.805	0.033	0.416	0.030	0.496	0.020	1.953	0.272	4.353	0.080
	FEM	0.699	0.052	0.831	0.038	0.425	0.033	0.497	0.023	1.958	0.274	4.502	0.082
	Reddy [15]	0.715	0.044	0.749	0.039	0.447	0.029	0.495	0.022	1.953	0.272	4.555	0.082
	Diff, %	3.70	6.12	3.22	15.15	2.16	10.00	0.20	15.00	0.25	0.73	3.42	2.50

* $\bar{\sigma}_{xx}\left(a/2, b/2, h/2\right)$, $\bar{\sigma}_{yy}\left(a/2, b/2, h/2\right)$, $\bar{\sigma}_{xy}\left(a, b, -h/2\right)$

Table 1 contains nondimensionalized deflections and stresses for antisymmetric cross-ply laminates under different types of mechanical loads. Also the differences between analytical and finite element model are illustrated in percentage for each case. From these results, it can be concluded that, for the same laminate thickness, antisymmetric cross-ply laminates with four or more layers are more desirable than two layer laminates because of reduction in deflections and stresses. This behavior is due to the bending-stretching coupling coefficients (B_{ij}) which are dominant in case of two layers.

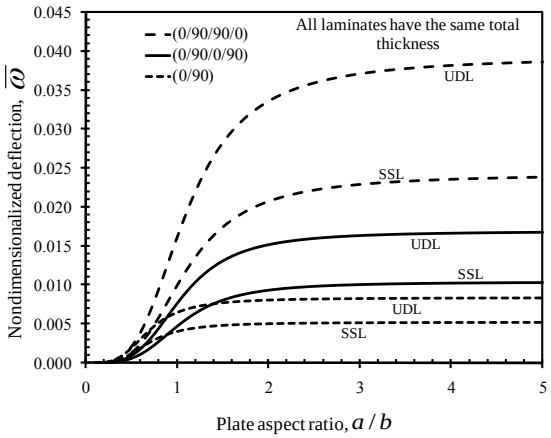

Fig. 2 Nondimensionalized center transverse deflection versus plate aspect ratio of simply supported (SS-1) laminates

Fig. 2-4 shows the effect of bending-stretching coupling and plate aspect ratio on the transverse deflection and stresses for a given z_0 under various types of mechanical loads. For comparison, results of symmetric laminates are also included.

The magnitude of deflections and stresses of symmetric laminates (0/90/90/0) are about two to three times that of antisymmetric (0/90/0/90) laminates for $a/b > 1$. For the uniformly distributed load there corresponds an aspect ratio, around $a/b = 2.25$ for $(0/90)_2$ and $a/b = 3.5$ for $(0/90)_s$ for which the deflection is the maximum of all aspect ratios. The effect of coupling coefficients is to increase the stresses. These coupling coefficients decrease in magnitude with the increase in the number of layers in antisymmetric cross-ply laminates and the laminate essentially behaves like an especially orthotropic plate. The dependence of the coupling effect on the modulus ratio is illustrated in Fig. 5 for SSL and UDL.

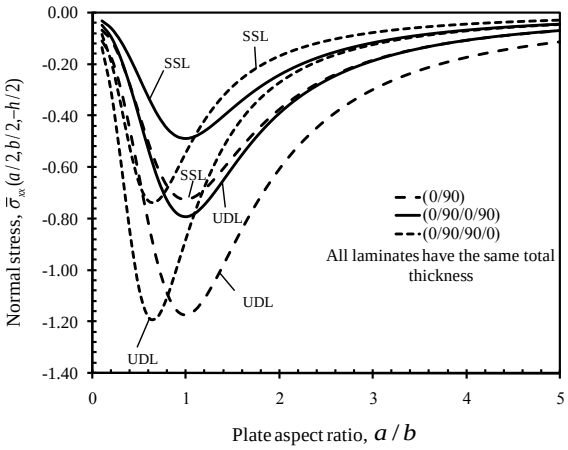

Fig. 3 Nondimensionalized normal stress versus plate aspect ratio of simply supported (SS-1) laminates

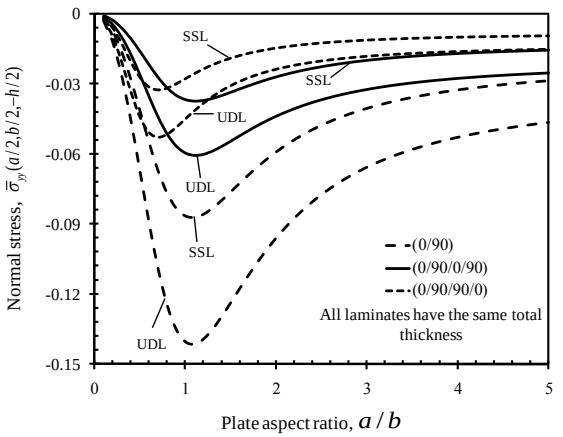

Fig. 4 Nondimensionalized normal stress versus plate aspect ratio of simply supported (SS-1) laminates

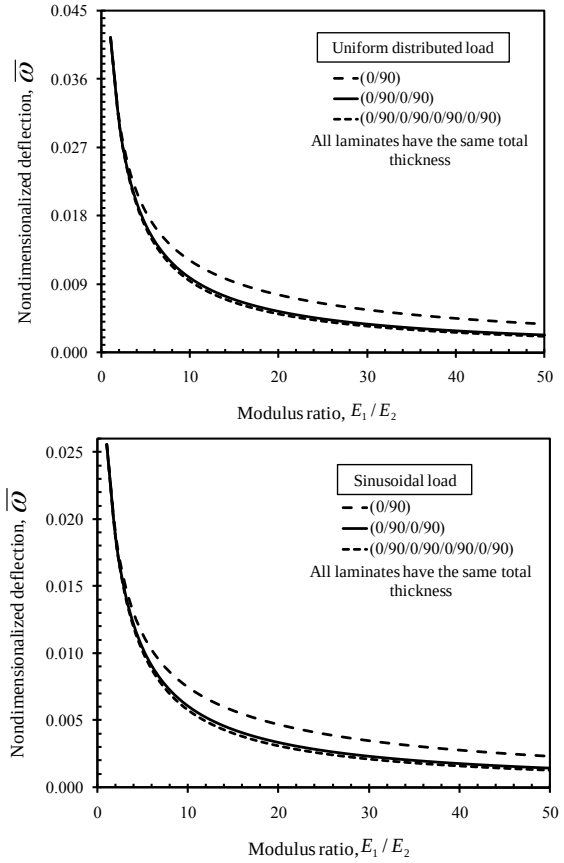

Fig. 5 Nondimensionalized center transverse deflection versus modulus ratio for simply supported cross-ply laminates under two types of loads

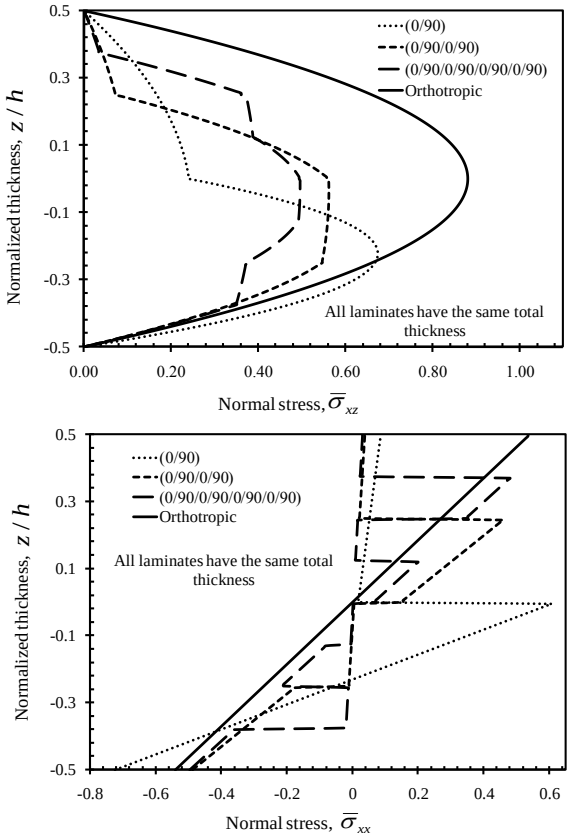

Fig. 6 Nondimensionalized maximum normal stress and transverse shear stress versus plate thickness under sinusoidal loading (SSL)

Distribution of the nondimensionalized maximum normal stress and transverse shear stress is shown in Fig. 6. These components are calculated through the thickness of antisymmetric cross-ply and orthotropic laminates under sinusoidal loadings.

The stress concentration is reduced in eight-layer cross-ply laminates than the two-layer one. So the latter plates experience larger stresses. Thus, the effect of the bending-stretching coupling present in two-layer plates on stresses is to increase the magnitude of stresses.

As discussed before, one of the lamination scheme which admits Navier solution for simply supported boundary conditions (SS-2) is antisymmetric angle-ply which is selected in this study. The effect of bending-extension coupling and the dependence of the coupling on the modulus ratio can be seen from the deflections and stresses presented in Table 2 for antisymmetric angle ply laminates $(-45/45)_k$ for $k = 1$, 2, and 4, and subjected to center point load and uniformly distributed load. For each case, differences between analytical and finite element method is also calculated in percentage.

Table 2

Transverse deflections and stresses in square laminates subjected to uniformly distributed transverse load (UDL) and central point load (CPL)*

$(-45/45)_k$		UDL				CPL			
		$\frac{E_1}{E_2}=10$		$\frac{E_1}{E_2}=20$		$\frac{E_1}{E_2}=10$		$\frac{E_1}{E_2}=20$	
		$\bar{\omega}\times10^2$	$\bar{\sigma}_{xx}$	$\bar{\omega}\times10^2$	$\bar{\sigma}_{xx}$	$\bar{\omega}\times10^2$	$\bar{\sigma}_{xx}$	$\bar{\omega}\times10^2$	$\bar{\sigma}_{xx}$
k = 1	Analytical	1.818	0.307	1.205	0.354	5.473	0.202	4.059	0.136
	FEM	1.822	0.311	1.214	0.355	5.481	0.211	4.060	0.141
	Reddy [15]	1.759	0.308	1.190	0.340	-	-	-	-
	Diff, %	0.220	1.280	0.750	0.280	0.140	4.450	0.02	3.670
k = 2	Analytical	1.161	0.221	0.621	0.217	3.852	0.158	2.272	0.088
	FEM	1.172	0.230	0.622	0.221	3.872	0.171	2.274	0.092
	Reddy [15]	0.999	0.214	0.542	0.205	-	-	-	-
	Diff, %	0.940	4.070	0.160	1.84	0.520	8.220	0.08	4.540
k = 4	Analytical	1.053	0.220	0.469	0.192	3.586	0.155	2.047	0.084
	FEM	1.058	0.229	0.473	0.195	3.590	0.167	2.051	0.087
	Reddy [15]	0.902	0.211	0.477	0.202	-	-	-	-
	Diff, %	0.470	4.090	0.850	1.560	0.110	7.740	0.190	3.570

* $\bar{\sigma}_{xx}(a/2,b/2,h/2)$, $\bar{\sigma}_{yy}(a/2,b/2,h/2)$, $\bar{\sigma}_{xy}(a,b,-h/2)$

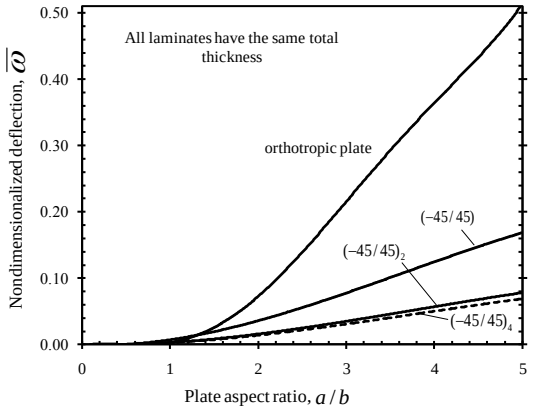

Fig. 7Nondimensionalized maximum transverse deflection versus plate aspect ratio under sinusoidal loading (SSL)

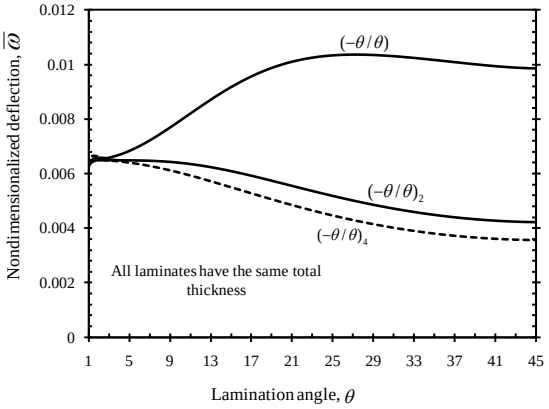

Fig. 8 Nondimensionalized maximum transverse deflection versus lamination angle for antisymmetric angle-ply laminates under sinusoidal load

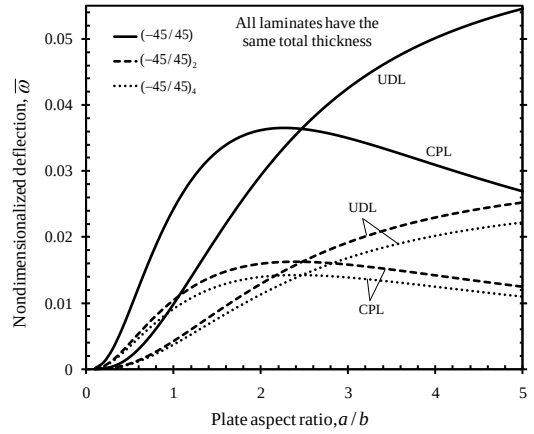

Fig. 9 Nondimensionalized maximum transverse deflection versus plate ratio for antisymmetric angle-ply laminates under different types of loading

Fig. 7 contains a plot of the nondimensionalized deflection versus plate aspect ratio for simply supported (SS-2) antisymmetric angle-ply laminates $(-45/45)_k$ under sinusoidal load. Orthotropic plate is also included for comparison. Fig. 8 contains $\bar{\omega}$ as a function of the lamination angle θ for square laminates $(-\theta/\theta)_k$ under sinusoidal load. The material properties used are the same as previous. Clearly, the bending-extension coupling is quite significant for two-layered plates, but the coupling decrease very rapidly as the number of layers is increased. Trend of changing $\bar{\omega}$ is for a two-layer plate is different from four and eight layer ones. Two layer angle-ply laminates have increasing trend versus variation of lamination angle while this behavior is decreasing for four and eight layer plates. Maximum deflection takes place for lamination angle of about 27° for two-layer plates. Also the magnitude of deflections of orthotropic laminates was about two to three times that of antisymmetric angle-ply laminates for $a/b > 3$ under sinusoidal loading.

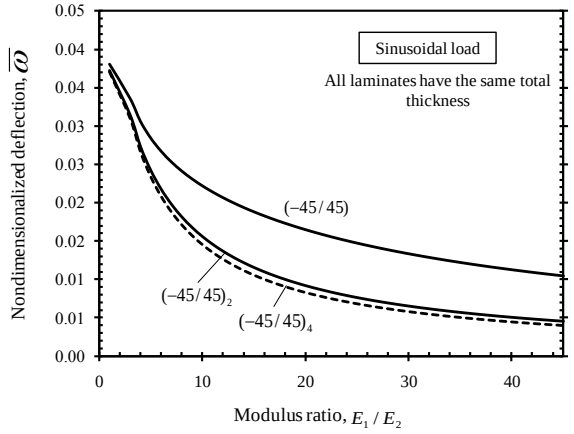

Fig. 10 Nondimensionalized center transverse deflection versus modulus ratio for simply supported angle-ply laminates under sinusoidal loads

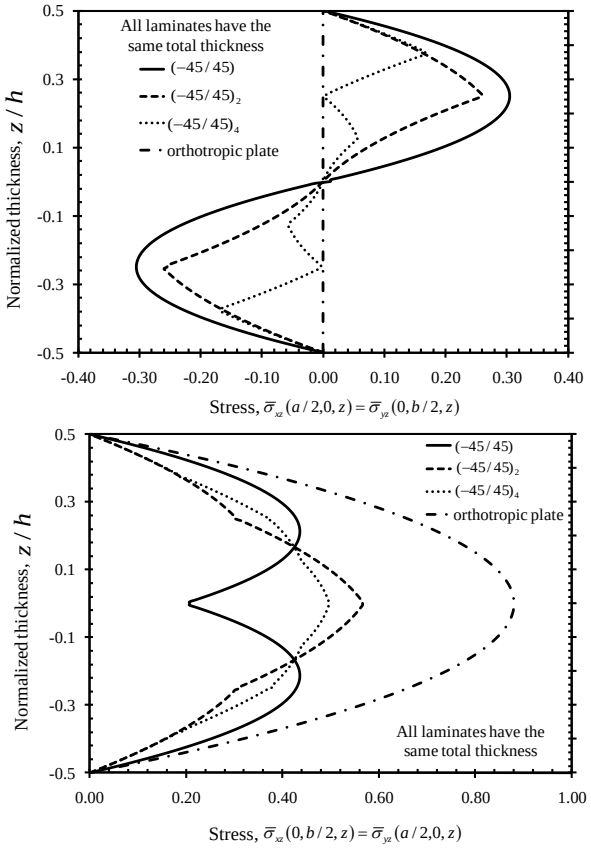

Fig. 11 Nondimensionalized maximum transverse shear stress versus plate thickness under sinusoidal loading (SSL)

Distribution of nondimensionalized transverse deflection versus plate aspect ratio for different types of loading are plotted in Fig. 9. From these results, it can be concluded that, for the same laminate thickness, antisymmetric

angle-ply laminates with four or more layers are more desirable than two layer laminates because of reduction in deflections and stresses. This behavior is due to the bending- extension coupling coefficients which are dominant in case of two layers.

Lastly, nondimensionalized transverse deflections as a function of the modulus ratio for square laminates under sinusoidal transverse load are presented in Fig. 10. The effect of coupling is significant for all modulus ratios except for those close to unity.

Distribution of the nondimensionalized transverse shear stress is shown for multi layer antisymmetric angle-ply and orthotropic laminates under sinusoidally distributed transverse loads in Fig. 11. Unlike in antisymmetric cross-ply laminates, the stress $\bar{\sigma}_{xz}$ is not zero at $(x, y) = (a/2, 0)$, although small in magnitude compared to that at $(x, y) = (0, b/2)$. Note that through-thickness variations are significantly altered when the number of layers is increased (for the same total laminate thickness).

3.2. Thermal loading

In the case of thermal loading, thermal properties of composite plates are assumed as:

$$\alpha_{11} = 6\times10^{-6}\ 1/^{\circ}\mathrm{C},\quad \alpha_{22} = 27\times10^{-6}\ 1/^{\circ}\mathrm{C}. \tag{40}$$

Also two types of thermal loads including uniform and linear distributed temperature through the thickness are considered as follows:

$$\left.\begin{array}{l}\text{uniform distributed temperature } (\mathrm{UDT}):\\ \Delta T(x,y,z) = T_0(x,y);\\ \text{linear distributed temperature } (\mathrm{LDT}):\\ \Delta T(x,y,z) = T_0(x,y) + zT_1(x,y),\end{array}\right\} \tag{41}$$

where T_0 and T_1 are assumed to be 100 and 10°C respectively. Stress free temperature is assumed T = 0°C.

In numerical results, nondimensionalized parameters for thermal loading are:

$$\left.\begin{array}{l}\text{deflection: } \bar{\omega} = \left(\omega\, E_2\, h^3/T^3\, a^4\right);\\ \text{shear stress: } \bar{\sigma}_{xz} = \left(100a\sigma_{\mathrm{xz}}/E_1T\alpha_{11}\, h\right);\\ \text{transverse stress: } \bar{\sigma}_{yy} = \left(10\sigma_{\mathrm{yy}}/E_1T\alpha_{11}\right);\\ \text{longitudinal stress: } \bar{\sigma}_{xx} = \left(10\sigma_{\mathrm{xx}}/E_1T\alpha_{11}\right).\end{array}\right\} \tag{42}$$

In thermal loading, because of the presented results were not found in the open literature, all predictions are compared with results of commercial finite element code ANSYS. Table 3 listed results of transverse deflections and stresses in square laminates subjected to uniformly and linear distributed temperature in thermal loads which are compared with finite element outputs. Also the difference between these two methods is reported in percentage for better evaluation of the results.

Table 3

Transverse deflections and stresses in square laminates subjected to UDT and LDT*

$(0/90)_k$		UDT				LDT			
		$\bar{\omega}$	$\bar{\sigma}_{xx}$	$\bar{\sigma}_{yy}$	$\bar{\sigma}_{xy}$	$\bar{\omega}\times10^2$	$\bar{\sigma}_{xx}$	$\bar{\sigma}_{yy}$	$\bar{\sigma}_{xy}$
k = 1	Analytical	0.087	0.129	1.516	0.936	0.234	1.826	1.752	0.382
	FEM	0.088	0.132	1.518	0.968	0.236	1.828	1.755	0.384
	Diff, %	1.140	2.320	0.130	3.410	0.850	0.100	0.170	0.520
k = 2	Analytical	0.020	0.480	1.473	0.431	0.109	1.732	1.732	0.392
	FEM	0.022	0.484	1.475	0.433	0.112	1.739	1.737	0.395
	Diff, %	10.00	0.830	0.130	0.690	2.750	0.400	0.280	0.760
k = 4	Analytical	0.009	0.568	1.467	0.436	0.107	1.732	1.730	0.393
	FEM	0.010	0.571	1.472	0.439	0.108	1.732	1.731	0.395
	Diff, %	11.11	0.520	0.340	0.680	0.930	0.000	0.050	0.500

* $\bar{\sigma}_{xx}(a/2, b/2, h/2)$, $\bar{\sigma}_{yy}(a/2, b/2, h/2)$, $\bar{\sigma}_{xy}(a, b, -h/2)$

Figs. 12 and 13 show the distribution of transverse shear stress through the thickness of the composite plates under different types of distributed temperature in thermal loading. For comparison, results of orthotropic laminates are also included.

In the case of eight-layer laminates, minimum stress concentration was found for both linear and uniform distributed temperature. Only difference is that for linear distributed temperature, the normal transverse shear stresses are not zero in bottom of the plates which is due to different temperatures at top and bottom of the plates.

Distribution of normal stresses through the thickness of bending-stretching coupling for a given z_0 is compared for various types of thermal loadings (UDT and LDT) in Fig. 14.

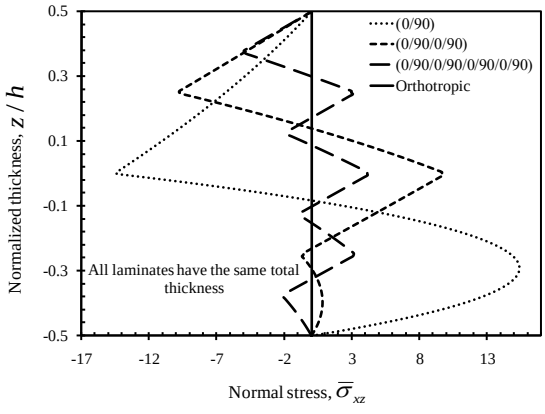

Fig. 12 Nondimensionalized maximum transverse shear stress versus plate thickness under UDT

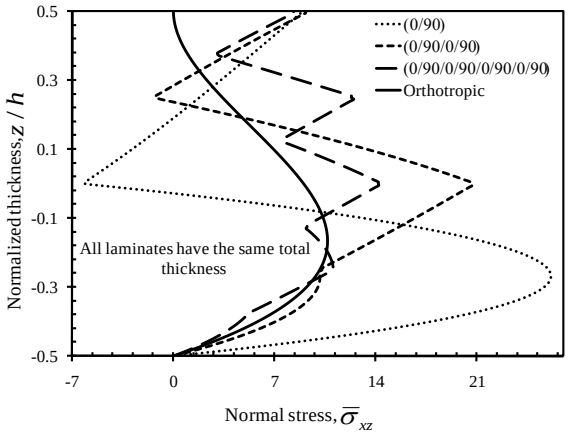

Fig. 13 Nondimensionalized maximum transverse shear stress versus plate thickness under LDT

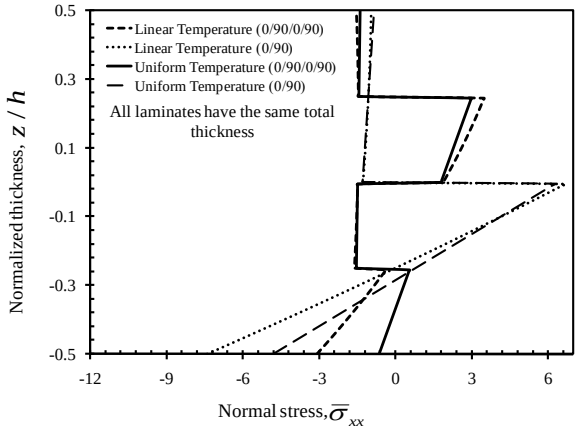

Fig. 14 Comparison of nondimensionalized maximum normal stresses versus plate thickness under uniform and LDT

Also variation of transverse deflection versus plate aspect ratios for linear distributed temperatures is illustrated in Fig. 15. It can be concluded that, magnitude of maximum transverse deflection for two-layer cross ply is about three or four times greater than four-layer type. Thus, the effect of the bending-stretching coupling present in two-layer plates on transverse deflection is to increase the magnitude of deflection.

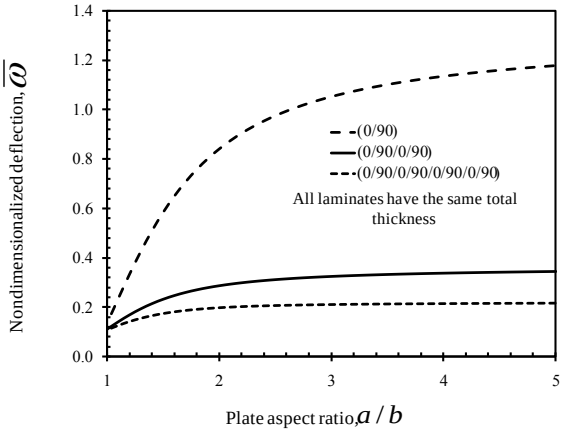

Fig. 15 Distribution of transverse deflection versus plate aspect ratios for linear distributed temperatures

4. Conclusions

Navier solution was applied using classical laminated theory to analysis cross-ply and angle-ply composite laminated plates with simply supported boundary conditions. Laminates were considered under different types of mechanical and thermal loads. For mechanical analysis, sinusoidal, uniform distributed and center point loads and in the case of thermal loadings, uniform and linear distributed temperatures were used. Results which was not found in open literature, were compared with commercial finite element analysis ANSYS. Following comments can be highlighted:

1. It can be concluded that for the same laminate thickness, antisymmetric laminates with four or more layers were more desirable than two layer laminates because of reduction in deflections and stresses for all cases. This behavior was due to the bending-stretching coupling coefficients for cross-ply and bending-extension coupling coefficients for angle-ply laminates, which was dominant in case of two layers.

2. Also the magnitude of deflections and stresses of symmetric cross-ply laminates was about two to three times greater than that of antisymmetric cross-ply laminates for $a/b > 1$ under sinusoidal loading. These ratios in case of uniform distributed loads were 2.25 and 3.5 for symmetric and unsymmetrical cross-ply laminates respectively.

3. The effect of coupling coefficients is to increase the stresses. These coupling coefficients decrease in magnitude with the increase in the number of layers in antisymmetric cross-ply laminates and the laminate essentially behaves like an especially orthotropic plate.

4. Maximum transverse shear stress is reduced by increasing number of layer in cross-ply laminates. So that maximum shear stress in eight-layer laminates decreased about two times in compare with orthotropic plates.

5. Maximum deflection takes place for lamination angle of about 27° for two-layer plates. Also the magnitude of deflections of orthotropic laminates was about two to three times that of antisymmetric angle-ply laminates for $a/b > 3$ under sinusoidal loading.

6. Unlike in antisymmetric cross-ply laminates, the stress $\bar{\sigma}_{xz}$ is not zero at $(x, y) = (a/2, 0)$, although small in magnitude compared to that at$(x, y) = (0, b/2)$. Note that through-thickness variations are significantly altered when the number of layers is increased (for the same total laminate thickness).

7. In the case of eight-layer laminates, minimum stress concentration was found for both linear and uniform distributed temperature. Only difference is that for linear distributed temperature, the normal transverse shear stresses are not zero in bottom of the plates which is due to different temperatures at top and bottom of the plates.

8. Finally it was found that in all cases, finite element outputs were in good agreement with theoretical analysis results.

References

1. **Zhang, C.; Di, S.; Zhang, N.** 2002. A new procedure for static analysis of thermo-electric laminated compo-

site plates under cylindrical bending, Composite Structures 56(2): 131-140.
http://dx.doi.org/10.1016/S0263-8223(01)00165-9.

2. **Shen Shen, H.** 2009. Nonlinear bending of functionally graded carbon nanotube-reinforced composite plates in thermal environments, Composite Structure 91(1): 9-19.
http://dx.doi.org/10.1016/j.compstruct.2009.04.026.
3. **Duc, N.D.; Minh, D.K.** 2010. Bending analysis of three-phase polymer composite plates reinforced by glass fibers and titanium oxide particles, Computational Materials Science 49(4): 194-198.
http://dx.doi.org/10.1016/j.commatsci.2010.04.016.
4. **Singh, B.N.; Lal, A.; Kumar, R.** 2008. Nonlinear bending response of laminated composite plates on nonlinear elastic foundation with uncertain system properties, Engineering Structures 30(4): 1101-1112.
http://dx.doi.org/10.1016/j.engstruct.2007.07.007.
5. **Sturzenbecher, R.; Hofstetter, K.** 2011. Bending of cross-ply laminated composites: An accurate and efficient plate theory based upon models of Lekhnitskii and Ren, Composite Structures 93(3): 1078-1088.
http://dx.doi.org/10.1016/j.compstruct.2010.09.020.
6. **Cetkovic, M.; Vuksanovic, D.J.** 2009. Bending, free vibrations and buckling of laminated composite and sandwich plates using a layerwise displacement model, Composite Structures 88(2): 219-227.
http://dx.doi.org/10.1016/j.compstruct.2008.03.039.
7. **Dash P.; Singh B.N.** 2010. Geometrically nonlinear bending analysis of laminated composite plate, Communications in Nonlinear Science and Numerical Simulation 15(10): 3170-3181.
http://dx.doi.org/10.1016/j.cnsns.2009.11.017.
8. **Andrade, L.G.; Awruch, A.M.; Morsch, I.B.** 2007. Geometrically nonlinear analysis of laminate composite plates and shells using the eight-node hexahedral element with one-point integration, Composite Structures 79(4): 571-580.
http://dx.doi.org/10.1016/j.compstruct.2006.02.022.
9. **Shiyekar, S.M.; Kant, T.** 2011. Higher order shear deformation effects on analysis of laminates with piezoelectric fiber reinforced composite actuators, Composite Structures 93(12): 3252-3261.
http://dx.doi.org/10.1016/j.compstruct.2011.05.016.
10. **Xiao, J.R.; Gilhooley, D.F.; Batra, R.C.; Gillespie, J.W.; McCarthy, M.A.** 2008. Analysis of thick composite laminates using a higher-order shear and normal deformable plate theory (HOSNDPT) and a meshless method, Composites Part B: Engineering 39(2): 414-427.
http://dx.doi.org/10.1016/j.compositesb.2006.12.009.
11. **Xu, R.; Wu, Y.F**. 2007. Two-dimensional analytical solutions of simply supported composite beams with interlayer slips, International Journal of Solids and Structures 44(1): 165-17.
http://dx.doi.org/10.1016/j.ijsolstr.2006.04.027.
12. **Kant, T.; Gupta, A.B.; Pendhari, S.S.; Desai, Y.M.** 2008. Elasticity solution for cross-ply composite and sandwich laminates, Composite Structures 83(1): 13-24.
http://dx.doi.org/10.1016/j.compstruct.2007.03.003.
13. **Kant, T.; Swaminathan, K.** 2002. Analytical solutions for the static analysis of laminated composite and sandwich plates based on a higher order refined theory, Composite Structures 56(4): 329-344.
http://dx.doi.org/10.1016/S0263-8223(02)00017-X.
14. **Mousavi, S.M.; Tahani, M.** 2012. Analytical solution for bending of moderately thick radially functionally graded sector plates with general boundary conditions using multi-term extended Kantorovich method, Composites B: Engineering 43(3): 1405-1416.
15. **Reddy, J.N.** 2003. Mechanics of Laminated Composite Plates and Shells: Theory and Analysis, second edition, 856.

M. A. Torabizadeh, A. Fereidoon

SKIRTINGŲ TIPŲ PAPRASTŲ KOMPOZICINIŲ LAMINATŲ, VEIKIAMŲ TERMOMECHANINIŲ NAVJĖ LENKIMO APKROVŲ, TYRIMAI

R e z i u m ė

Remiantis klasikine laminuotų plokštelių teorija (KLPT), atliktas analitinis ir skaitinis įvairių mechaninių ir terminių apkrovų veikiamų paprastai laminuotų plokštelių tyrimas. Įvertintas šių plokštelių skersinis ir sukamasis poslinkis. Atsižvelgiant į tai, Navjė metodas pritaikytas paprastai atremtai stačiakampei laminuotai plokštelei, o baigtinių elementų kodas, naudojant ANSYS programą, pritaikytas gauto sprendinio tikslumui nustatyti. Taip pat yra ištirta kompozicinių laminuotų plokštelių laminavimo schemos, temperatūros, geometrijos ir mechaninių savybių įtaka esant statinei lenkimo apkrovai. Gauti rezultatai gerai sutapo su pateiktais literatūroje.

M.A. Torabizadeh, A. Fereidoon

NAVIER-TYPE BENDING ANALYSIS OF GENERAL COMPOSITE LAMINATES UNDER DIFFERENT TYPES OF THERMOMECHANICAL LOADING

S u m m a r y

An analytical and numerical solution for general laminated composite plates under different types of mechanical and thermal loading is presented based on classical lamination plate theory (CLPT). General lamination was evaluated by assumption of cross-ply and angle-ply laminated plates. In order to this, Navier-type method is applied for simply supported rectangular laminates and a finite element code using ANSYS is also developed to investigate the accuracy of the presented solution. Effects of lamination scheme, temperature service, geometry ratio and mechanical properties of composite laminates on static bending of laminated composite are also investigated and good agreement is found between evaluated results and those available in open literature.

Keywords: Navier-type, composite plates, mechanical loading, thermal effects.

Received June 05, 2012
Accepted August 21, 2013